Bulat et al., http://www.jcb.org/cgi/content/full/jcb.201305134/DC1

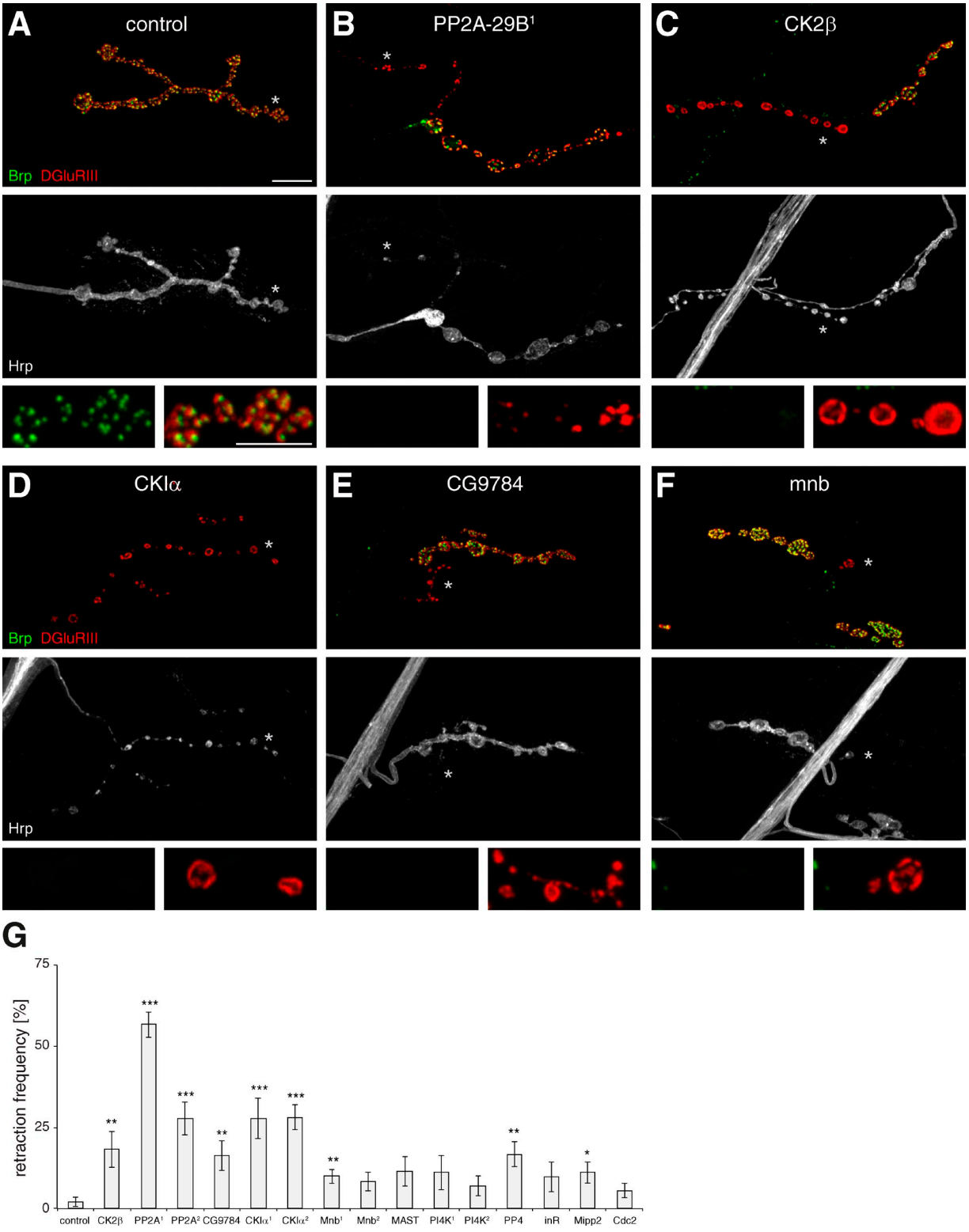

Figure S1. **RNAi screen identifies kinases and phosphatases essential for synapse stability.** (A–F) NMJs on muscle 4 were stained for the presynaptic active zone marker Brp (green), postsynaptic glutamate receptors (DGluRIII, red), and the presynaptic membrane marker Hrp (white). (A) A stable wild-type NMJ on muscle 4 as indicated by the precise apposition of pre- and postsynaptic markers throughout the nerve terminal. (B–F) RNAi-mediated knockdown of the indicated kinases or phosphatases caused synaptic retractions characterized by the presence of postsynaptic glutamate receptor clusters despite the absence of the presynaptic active zone marker Brp. At these sites, the presynaptic membrane (white) was no longer continuous and only membrane remnants were visible opposite postsynaptic glutamate receptors. The severity of the synaptic retraction phenotype ranged from single unopposed postsynaptic profiles (F) to the entire elimination of all presynaptic markers (D). Bars: (main panels) 10 µm; (enlarged panels below) 5 µm. (G) Quantification of synaptic retraction frequency (*, $P \leq 0.05$; **, $P \leq 0.01$; ***, $P \leq 0.001$; n = 9–15 animals, muscle 4). Error bars represent SEM.

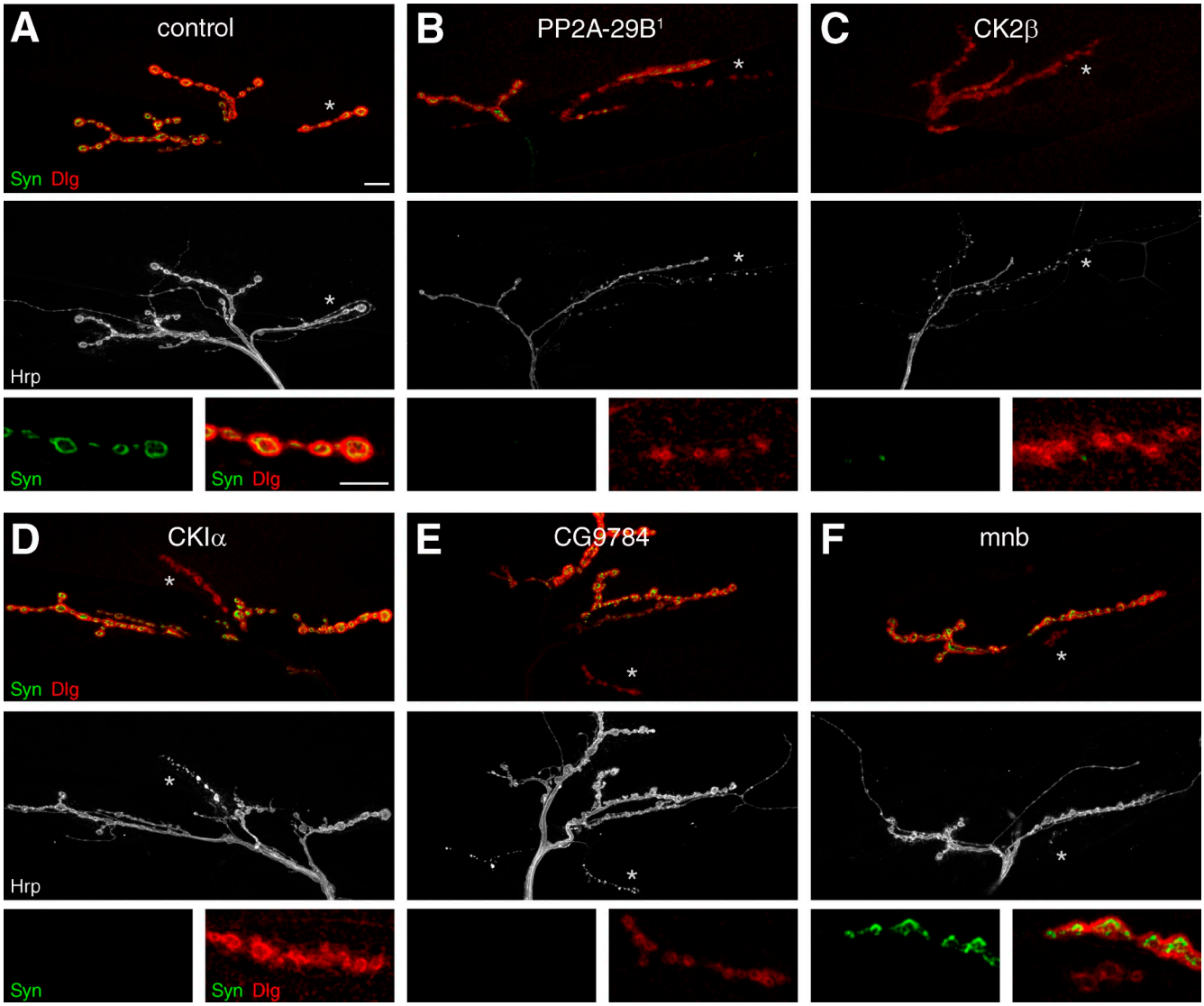

Figure S2. **RNAi screen identifies kinases and phosphatases essential for synapse stability.** (A–F) NMJs on muscles 1/9 were stained for the presynaptic vesicle marker synapsin (Syn, green), the postsynaptic SSR marker Dlg (red), and the presynaptic membrane marker Hrp (white). (A) A stable wild-type NMJ on muscles 1/9 as indicated by the precise apposition of pre- and postsynaptic markers throughout the nerve terminal. (B–F) RNAi-mediated knockdown of the denoted kinases or phosphatases caused synaptic retractions indicated by the presence of the postsynaptic SSR marker Dlg, despite the absence of synaptic vesicles (Syn). At these sites, the presynaptic membrane (white) was no longer continuous and only membrane remnants were visible opposite postsynaptic Dlg. In addition, a reduction of the postsynaptic SSR marker Dlg was evident at these sites, which indicates the disassembly of postsynaptic structures. The severity of the synaptic retraction phenotype ranged from small retractions (F) to the entire elimination of all presynaptic markers (C). Asterisks indicate regions shown at high magnification. Bars: (main panels) 10 µm; (panels below) 5 µm.

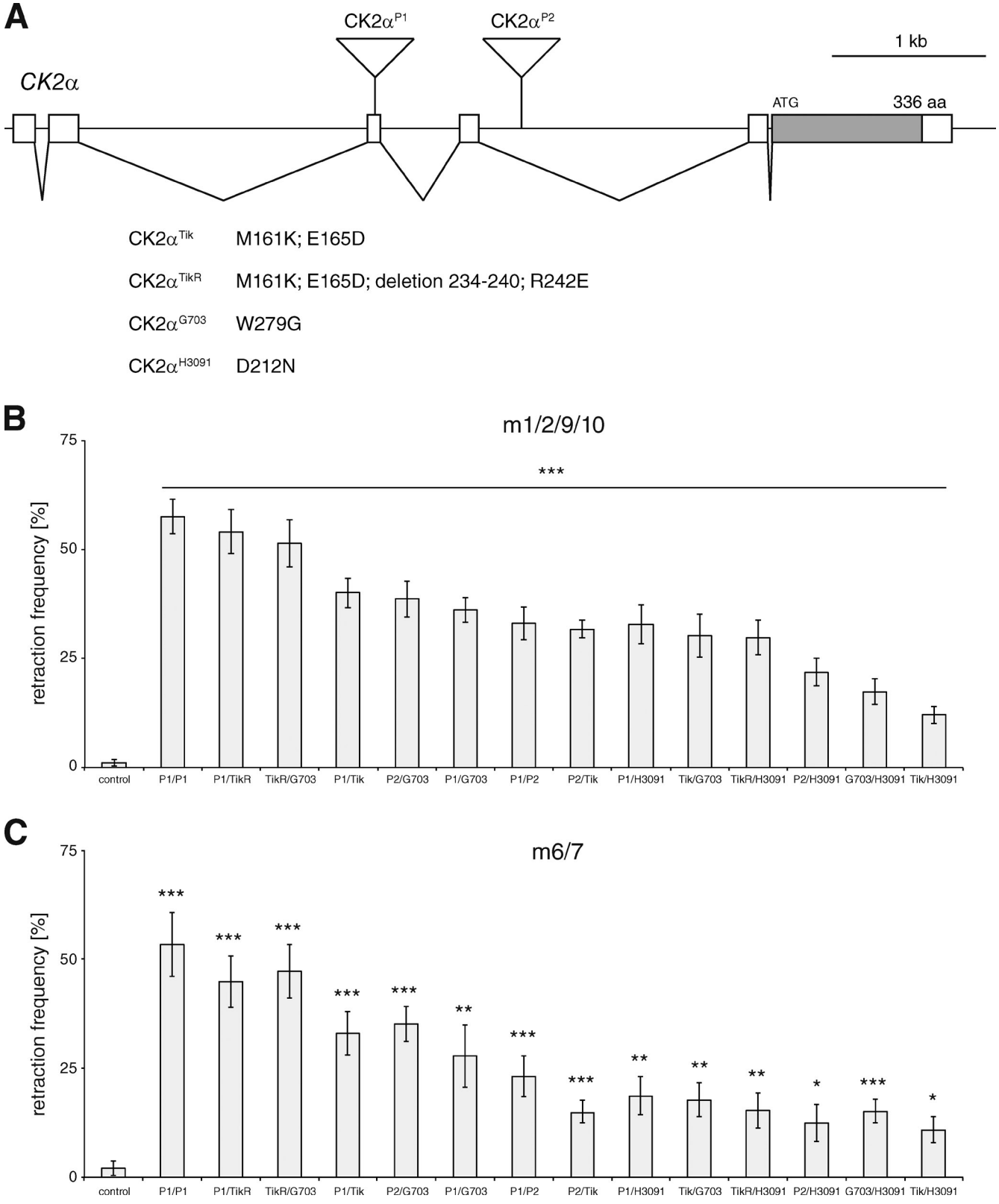

Figure S3. **Analysis of synaptic retractions in CK2α mutants.** (A) Schematic of the *CK2α* gene locus. Exons are denoted in white and the open reading frame in gray. The position of the PiggyBac insertion mutations $CK2\alpha^{P1}$ (PBac{SAstopDsRed}LL05896) and $CK2\alpha^{P2}$ (PBac{SAstopDsRed}LL07221) are indicated. The amino acid substitutions and/or deletions are denoted for ethyl methanesulfonate–induced *CK2α* alleles. (B and C) Quantification of synaptic retraction frequencies of all larval viable *CK2α* allelic combinations on muscles 1/9 and 2/10 (B) and muscles 6/7 (C). We observed a significant increase in the frequency of synaptic retractions for all allelic combinations compared with control animals. Synaptic retraction frequencies were slightly reduced at ventral compared with dorsal muscle groups. The relative phenotypic strength of the different allelic combinations remained identical (*, $P \leq 0.05$; **, $P \leq 0.01$; ***, $P \leq 0.001$; n = 9–21 animals). Error bars represent SEM.

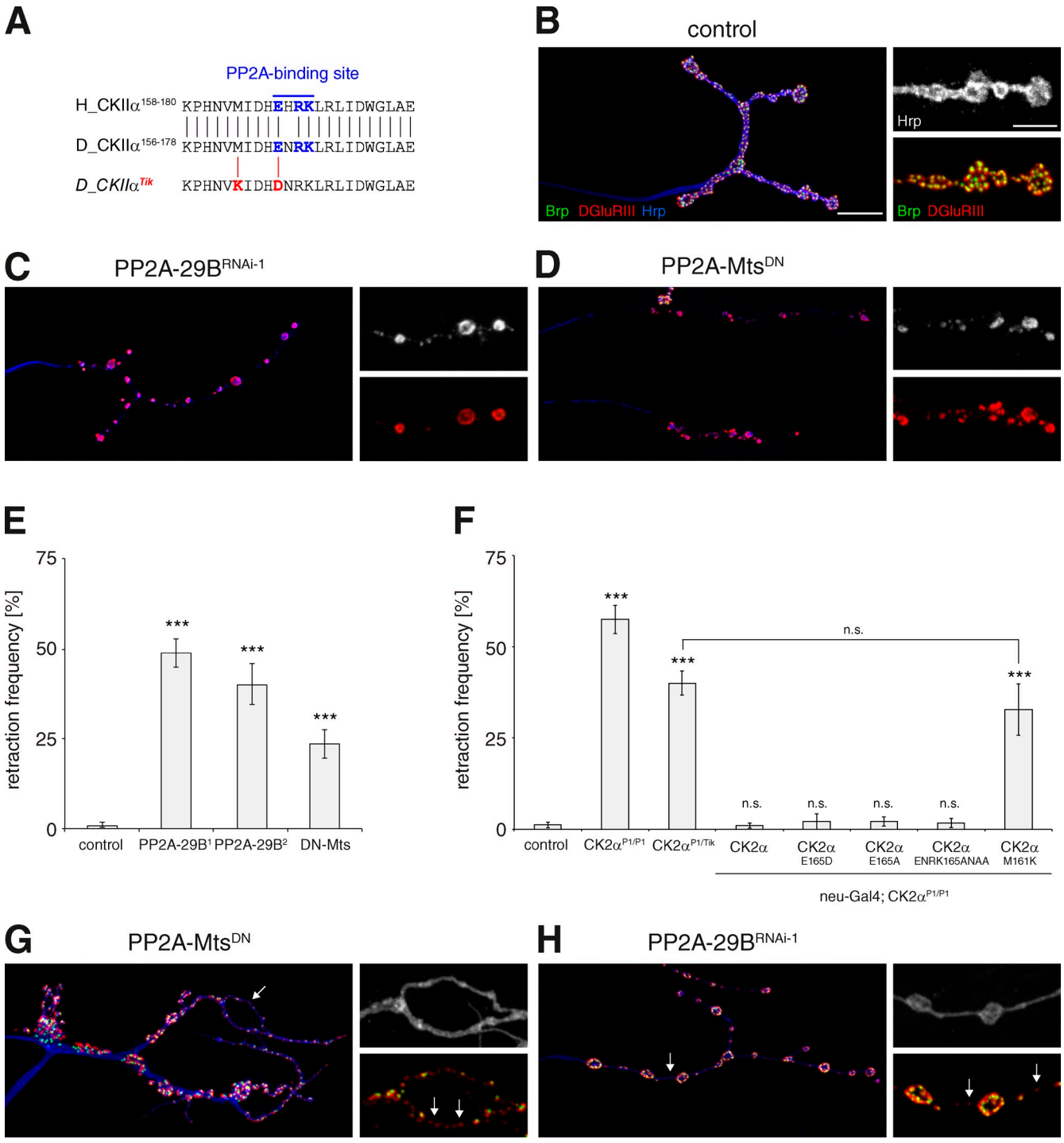

Figure S4. **CK2α–PP2A interaction is not essential for the control of synapse stability.** (A) Sequence comparison of the PP2A interaction domains of *Drosophila* and human CK2α. Amino acid residues mediating the CK2α–PP2A interaction are highlighted in blue. The amino acid exchanges of the *Drosophila CK2α*^{Tik} mutation are indicated in red (M161K, E165D). (B–D) NMJs on muscle 4 stained for the presynaptic active zone marker Brp (green), postsynaptic glutamate receptors DGluRIII (red), and the presynaptic motoneuron membrane marker Hrp (blue, white). (B) A stable wild-type NMJ is shown. (C) Knockdown of presynaptic PP2A resulted in severe synaptic retractions. (D) Impairing PP2A activity by expression of a dominant-negative version of the catalytic subunit Mts in motoneurons resulted in synaptic retractions, as indicated by loss of the presynaptic marker Brp and fragmentation of the presynaptic membrane (Hrp). (E) Quantification of synaptic retractions of two independent PP2A-29B RNAi lines and dnMts. (F) Analysis of the requirement of the CK2α–PP2A interaction for synapse stability. Expression of wild-type CK2α, CK2α^{E165D}, CK2α^{E165A}, and CK2α^{ENRK165ANAA} but not of CK2α^{M161K} was sufficient to restore synapse stability in *CK2α* mutant animals (***, $P \leq 0.001$; muscles 1/9, 2/10). Error bars represent SEM. (G) Presynaptic expression of dominant-negative Mts resulted in synapse formation defects, indicated by postsynaptic glutamate receptor clusters not yet opposed by Brp (arrows, enlarged panel to the right). The continuous membrane staining demonstrates that these events do not represent synaptic retractions. The sites of delayed synapse formation were often in areas characterized by long, protrusion-like membrane extensions (arrow). (H) Knockdown of presynaptic PP2A-29B caused less-severe synapse formation defects (arrows, enlarged panel to the right). Bars: (main panels) 10 µm; (enlarged panels on the right) 5 µm.

Table S1 lists all kinases and phosphatases and their VDRC number analyzed in the RNAi screen, and is available as an Excel file.

Table S2 lists all data displayed in Figs. 1–8 and Figs. S1–S4, and is available as a PDF.